COVID 19 breakthrough infection risk: a simple physical model describing the dependence on antibody concentration

David E Williams

School of Chemical Sciences, University of Auckland, Private Bag 92019, Auckland, 1142, New Zealand

Email: David.williams@auckland.ac.nz

Abstract

The empirically-observed dependence of SARS-CoV-2 vaccine efficacy on antibody concentration has a rational explanation in the statistics of binding of antibody to spike proteins on the virus surface: namely that the probability of protection is the probability of antibody binding to more than a critical number of the spike proteins protruding from the virus. The model is consistent with the observed antibody concentrations required to induce immunity.

Key words

SARS-CoV-2 immunity, vaccine efficacy, antibody concentration, binding statistics

Introduction

The concentration in blood of IgG antibodies against the spike receptor binding domain of the SARS-CoV-2 virus is well correlated with neutralisation efficacy against the virus [1] and appears to be a useful predictor of breakthrough infection risk for vaccinated or convalescent individuals [2, 3]. The well-documented increase in breakthrough infection risk over time for some months following vaccination [4-7] has been attributed to a decrease in IgG concentration, in advance of the development later of cell-based immunity [5, 7-9]. An empirical model for this dependence has been given[10, 11] and developed into a model describing breakthrough infection risk, and importation risk stratification using quantitative serology [12]. Since the risk model relies heavily on the empirical correlation of vaccine efficacy with neutralising antibody concentration, it would be useful to find a physical basis for the correlation and to use this to perhaps develop more confidence in the risk prediction.

In the following, a simple model for the immune response is developed. The mechanism of antibody neutralisation of viral infection is complex and depends on the type of virus [13, 14]. Given current knowledge that vaccine efficacy is (at least for some months) determined by the concentration of neutralizing antibodies, is assumed that the mechanism is simply antibody binding to the spike

protein blocking the virus binding to host cells [13, 15]. Potent antibodies indeed block binding of the virus to its receptor [16].

Model

Let *N* denote the total number of spikes per virus particle. The number is variable from one particle to another, distributed over the range 10 – 40 with median around 25 [17, 18] . Let *s* denote the number of antibody molecules bound on a particular particle. We suppose that there is some threshold number of sites, ($N - s^*$) that must be unoccupied in order that there is a significant probability that a virus particle may bind to and infect a cell. We therefore wish to calculate the probability that the number of occupied sites is greater than or equal to s*, $P(s \geq s^*)$, as a function of the antibody concentration in the medium surrounding the virus particle.

The question is therefore : what is the probability distribution for the number of antibody molecules bound per particle. The system can be represented by a state diagram:

$$0 \underset{\lambda_2}{\overset{\lambda_1}{\rightleftarrows}} 1 \rightleftarrows 2 \rightleftarrows \ldots\ldots\ldots\ldots \rightleftarrows s \rightleftarrows \ldots.$$

where λ_1 denotes the frequency of adsorption of molecules to a particular particle and λ_2 the frequency of desorption. A simplifying assumption is that the diameter of the virus particle and number of spikes/particle are such that the spacing of the spikes is significantly larger than the antibody dimensions so lateral interactions between bound antibodies can reasonably be ignored. The objective is to calculate the probability of a given state for a particular particle.

The transition frequencies, λ_1 and λ_2 are dependent on the site occupancy: the rate of binding to a particle is proportional to the collision frequency of antibodies with unoccupied sites, hence dependent on the fraction of the particle area that is unoccupied, hence on the fraction of unoccupied sites, whilst the rate of desorption is proportional to the number of occupied sites. Hence for the exchange between state (*s*-1) and state *s*, where *c* denotes the solution concentration of antibody

$$\lambda_{1,s-1} = k_{on} c \left(1 - \frac{s-1}{N}\right)$$

$$\lambda_{2,s} = k_{off} s$$

The occupancy probability, *p(s,t)* , is determined as follows [19]:

[probability that occupancy of a particle is *s* at time *t*] =

[probability that the occupancy was *(s-1)* at *(t-δt)* and that one further antibody was captured in the interval *(t-δt)* to *t*]

+ [probability that the occupancy was *(s+1)* at *(t-δt)* and that one antibody was desorbed from the surface in the interval *(t-δt)* to *t*]

— [probability that the occupancy was at *s* at *(t-δt)* and that antibody was captured or lost in the interval *(t-δt)* to *t*]:

$$p(s,t) = p(s-1,t-\delta t)\lambda_{1,s-1}\delta t + p(s+1,t-\delta t)\lambda_{2,s+1}\delta t + p(s,t-\delta t)(1-\lambda_{1,s}\delta t - \lambda_{2,s}\delta t)$$

Hence, altering the notation : *p(s,t)* = p_s , and substituting for λ

$$\frac{dp_s}{dt} = p_{s-1}\lambda_{1,s-1} + p_{s+1}\lambda_{2,s+1} - p_s\left(\lambda_{1,s} + \lambda_{2,s}\right)$$

$$= p_{s-1}k_{on}c\left(1-\frac{s-1}{N}\right) + p_{s+1}k_{off}(s+1) - p_s\left(k_{on}c\left[1-\frac{s-1}{N}\right] + k_{off}s\right) \quad - \quad (1)$$

For the state 0, from which there is no antibody desorption,

$$\frac{dp_0}{dt} = p_1k_{off} - p_0k_{on}c \quad (2)$$

The initial condition is: *p*(0) = 1 at *t* = 0 and furthermore $\sum_{s=0}^{N} p_s = 1$ at any *t*.

The solution for the time-varying probabilities can be obtained numerically. The solution for the steady-state occupation probability is obtained by setting the derivatives to zero and solving recursively starting with the determination of p_1 from eq(2), applying eq (1) to obtain successively the p_s, and applying $\sum_{s=0}^{N} p_s = 1$ to obtain p_0.

Thus, defining $z = \frac{k_{on}c}{k_{off}}$ and $r_s = \left(\frac{1}{s!}\right)\left(\frac{N!}{N^s(N-s)!}\right)$ gives:

$$p_s = r_s z^s / \sum_{s=0}^{N} r_s z^s \quad (3)$$

If *N* is very large and the total occupancy is sufficiently small, then p_s follows a Poisson distribution: $p_s = \frac{z^s}{s!}exp(-z)$.

For arbitrary *N*,

$$P(s \geq s^*) = \sum_{s=s*}^{N} r_s z^s / \sum_{s=0}^{N} r_s z^s \quad (4)$$

The dimensionless concentration, *z*, is the ratio of the antibody solution concentration to the antibody affinity for the binding site.

Infection also requires some dose of virus be received. Suppose that the dose, *D*, across an exposed population is described by a probability distribution *P*(*D*) . Then, in the presence of antibody, within some dose, *D*, the number of virus particles that are infectious would be *P(s ≥ s*)D* . Suppose that a

'critical dose', D^*, is required to trigger an infection. The probability of infection would then be $\int_{D^*}^{\infty} P(D)\mathrm{d}D / \int_0^{\infty} P(D)\mathrm{d}D$. In the presence of antibody, the vaccine efficacy, E, = (number of infections amongst vaccinated people / number of infections amongst unvaccinated people) with exposure and transmission probability the same in each group, would be:

$$E = \int_{D^*}^{\infty} P(s \geq s^*)P(D)\mathrm{d}D / \int_0^{\infty} P(D)\mathrm{d}D = P(s \geq s^*) \int_{D^*}^{\infty} P(D)\mathrm{d}D / \int_0^{\infty} P(D)\mathrm{d}D \qquad (5)$$

That is, the dependence of vaccine efficacy on antibody concentration would be just the dependence of $P(s \geq s^*)$ on concentration, calculated according to equation (4).

Results and Discussion

Figure 1 shows the variation of $P(s \geq s^*)$ for various values of N and N-s^*. The line is fitted to the log-logistic function used by Khouri *et al* [11] empirically to derive the dependence of vaccine efficacy, E, on IgG concentration, c :

$$E = 1/\left[1 + \exp\left(-k(\ln c - \ln c_{50})\right)\right] = 1/[1 + (c_{50}/c)^k] = 1/[1 + (z_{50}/z)^k] \qquad (5)$$

Where the dimensionless concentration, z, has been substituted.

By attributing vaccine efficacy to the probability that more than a critical number of binding sites on the virus should be occupied by antibody, the statistical model captures this general behaviour and demonstrates the dependence of the critical parameter, z_{50} on the assumption made regarding the critical site coverage, s^*, and on the total number of binding sites / particle, N. Since z is proportional to antibody affinity, the model captures also the effect of this and attributes the difference between different vaccines to both the concentration and the affinity of the antibodies induced by vaccination. Figure 2 shows that the parameter z_{50} , interpretable as the median antibody concentration relative to affinity required to achieve 50% blocking, varies strongly both with the number of binding sites, N, and the threshold site occupancy required to cause blocking, s^*.

Khouri *et al* [11] give k = 0.87 with 95% confidence interval 0.96 – 1.82 . Figure 3 shows the variation of k determined for the statistical site-binding model for different values of the total number of sites, N, that span the range given for the SARS-CoV-2 virus [17, 18], and with different values assumed for the threshold number of sites left uncovered in order to induce infection, $N - s^*$. This number is unknown. It may be that virus binding to target requires multiple spike interactions, from spikes that are randomly separated, or may require adjacent spikes, or may be effective with just one spike uncovered. The infection may be 'land and stick' or 'land and seek' [20]. The probability that a collision between virus particle and cell is a reactive collision leading to infection would be different for each of these scenarios.

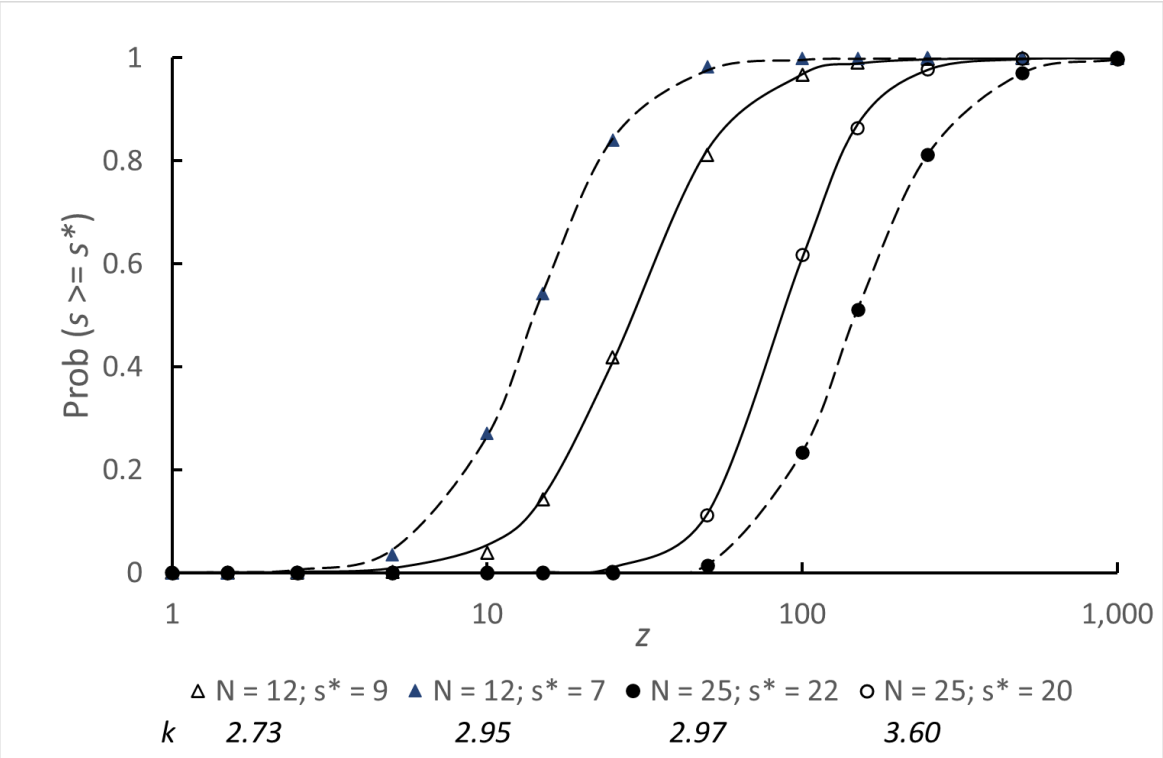

Figure 1 Probability of site occupancy, $s \geq s^*$, against dimensionless neutralising antibody concentration, z, for different numbers of spikes on the virus particle, N and various s^*; points are calculated and lines are fits to the log-logistic function, equation 5, with rate parameter k

The values of the rate parameter, k, deduced for different values of $N - s^*$ are rather higher than that deduced by Khouri *et al* , even for the most stringent neutralisation criterion, that only one site unblocked on the virus could lead to infection. There are two reasons that can be deduced. First, there is a distribution of binding site number. Second, It is known that an antibody population with a range of affinity is induced either by vaccination or by infection [1, 16, 21]. The induced affinity distribution may depend on the specific vaccine. The effect of a variation of the affinity distribution can straightforwardly be modelled by introducing a distribution of the parameter z_{50} , whose variation for a particular antibody concentration would be due to variation of antibody affinity.

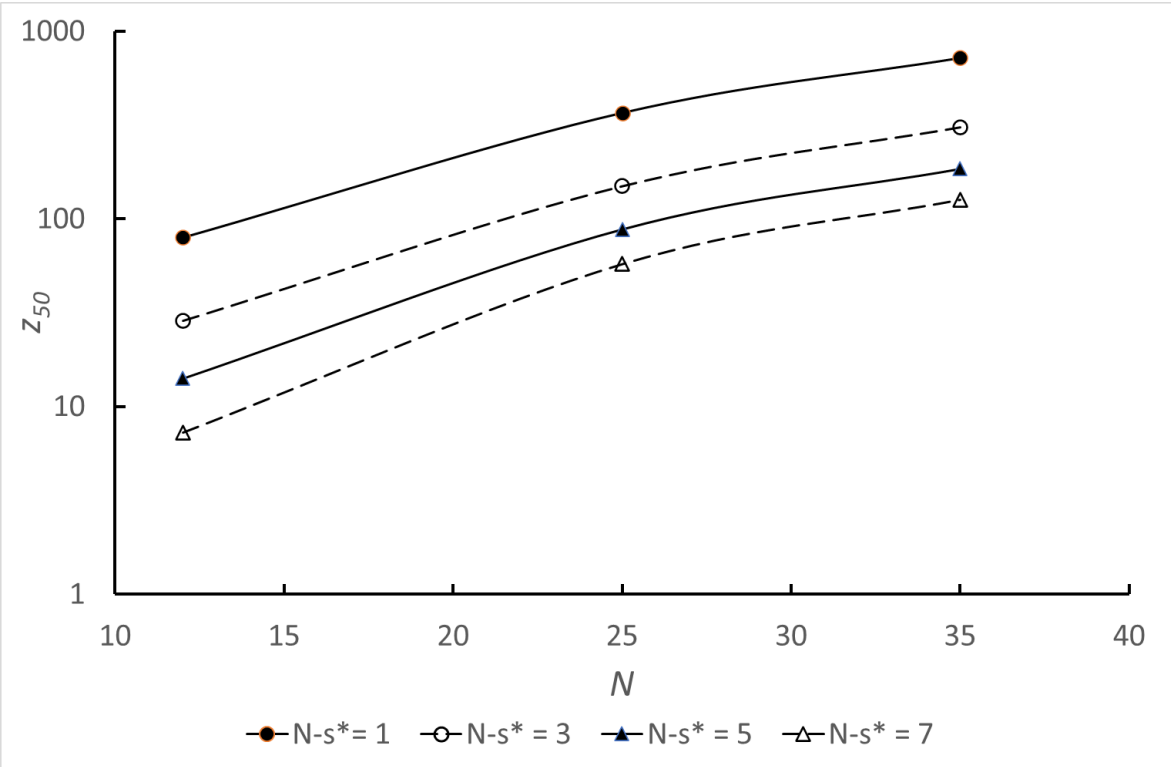

Figure 2 Variation of dimensionless median binding concentration, z_{50} (equation 5) with total binding site number, *N*, and threshold number of vacant sites to allow binding, *N - s**.

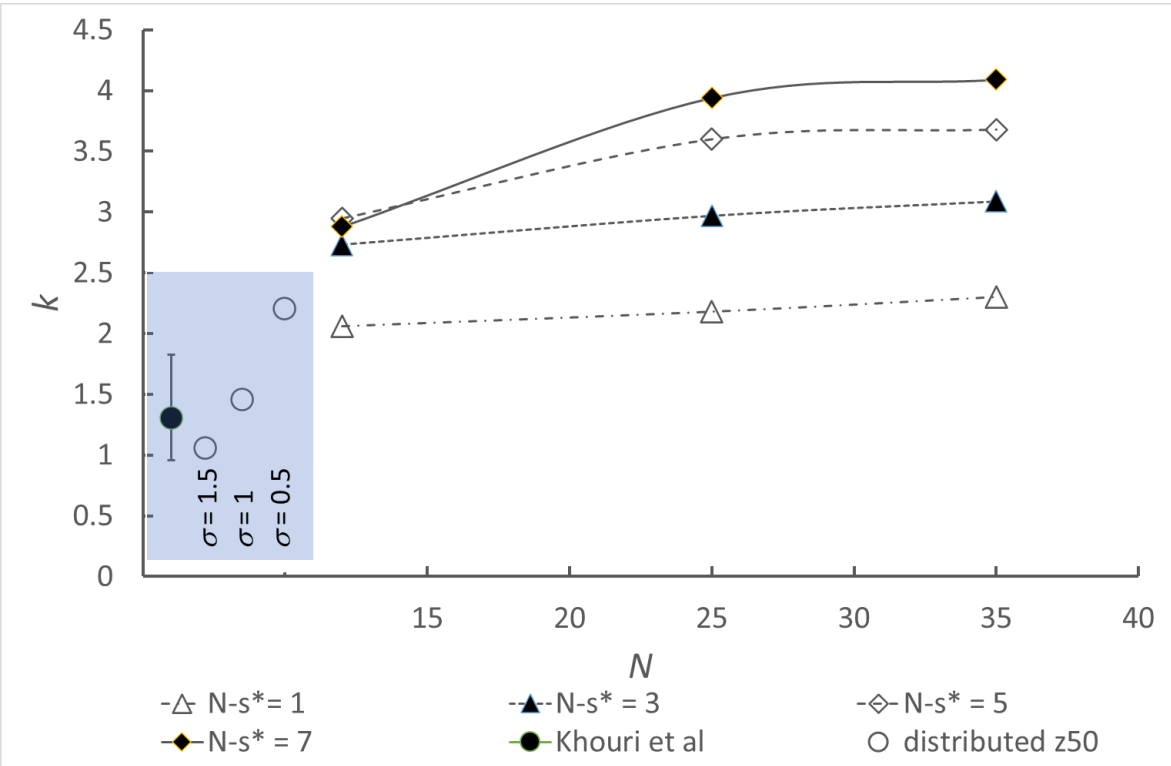

Figure 3. Rate parameter *k* of the log-logistic fit shown in Figure 1 against number of spikes on the virus particle, for different threshold numbers of unoccupied spikes, *N-s**. Symbols O : effect of introduction of a log-normal distribution of dimensionless concentration, *z*, equivalent to a distribution of neutralising antibody affinity, for spike number *N* = 25 and *N-s** = 3; σ is the log-normal standard deviation of affinity. Comparison with the fit of Khouri *et al*,[11] describing vaccine efficacy as a function of neutralising antibody concentration.

Figure 3 shows as a comparison the effect of introducing a log-normal distribution antibody affinity through a log-normal distribution of z_{50} . With a distribution that is of moderate broadness, the deduced value of *k* comes into the middle of the range given by Khouri *et al*. To come to the bottom of the range requires a very broad affinity distribution.

The magnitude scale for antibody concentration can be estimated, as a further qualitative check that the model is sensible. Figure 2 shows that a high degree of protection would require $z_{50} \sim 10^2 – 10^3$. Human antibodies induced in response to SARS-CoV-2 have a range of affinity (ratio of 'on' rate constant to 'off' rate constant, k_{on}/k_{off}) with the most potent ~10^{11} M [16], to the receptor binding domain. Thus, given the deduced range of z_{50} , the expected range of median antibody concentration would be ~$10^{-9} – 10^{-8}$ M. Literature data report results in a variety of units, and assay systems are not directly comparable (as can for example be seen by comparison of the concentration distributions over the same population measured by several different assays, reported by Ainsworth *et al*. [22]). Data from Roche [23] indicate median convalescent antibody concentration ~ 4 nM and from Wei *et al*.[24] post-vaccination concentrations in the range 200 – 500 ng / mL (1.5 – 3.5 nM assuming an antibody molecular weight of 150 kDa) whilst other studies (converting units) show concentrations above 10 nM [9 25]. The antibody concentration range deduced from the model therefore seems reasonable.

Conclusion

The empirically-observed dependence of vaccine efficacy on antibody concentration has a rational explanation in the statistics of binding of antibody to spike proteins on the virus surface. The model is consistent with the observed antibody concentrations required to induce immunity and with the observed dependence of vaccine efficacy on antibody concentration. It provides a way to constrain the value of the parameter describing the increase of vaccine efficacy with increase of antibody concentration and thus is a useful tool in the development of models to relate, for an individual person, risk of breakthrough infection given measured antibody concentration

1. Wang, Z. J.; Schmidt, F.; Weisblum, Y.; Muecksch, F.; Barnes, C. O.; Finkin, S.; Schaefer-Babajew, D.; Cipolla, M.; Gaebler, C.; Lieberman, J. A.; Oliveira, T. Y.; Yang, Z.; Abernathy, M. E.; Huey-Tubman, K. E.; Hurley, A.; Turroja, M.; West, K. A.; Gordon, K.; Millard, K. G.; Ramos, V.; Da Silva, J.; Xu, J. L.; Colbert, R. A.; Patel, R.; Dizon, J.; Unson-O'Brien, C.; Shimeliovich, I.; Gazumyan, A.; Caskey, M.; Bjorkman, P. J.; Casellas, R.; Hatziioannou, T.; Bieniasz, P. D.; Nussenzweig, M. C., mRNA vaccine-elicited antibodies to SARS-CoV-2 and circulating variants. *Nature* **2021,** *592* (7855), 616-+.
2. Gilbert, P. B.; Montefiori, D. C.; McDermott, A.; Fong, Y.; Benkeser, D. C.; Deng, W.; Zhou, H.; Houchens, C. R.; Martins, K.; Jayashankar, L.; Castellino, F.; Flach, B.; Lin, B. C.; O'Connell, S.; McDanal, C.; Eaton, A.; Sarzotti-Kelsoe, M.; Lu, Y.; Yu, C.; Borate, B.; van der Laan, L. W. P.; Hejazi, N.; Huynh, C.; Miller, J.; El Sahly, H. M.; Baden, L. R.; Baron, M.; De La Cruz, L.; Gay, C.; Kalams, S.; Kelley, C. F.; Kutner, M.; Corey, L.; Neuzil, K. M.; Carpp, L. N.; Pajon, R.; Follmann, D.; Donis, R. O.; Koup, R. A., Immune Correlates Analysis of the mRNA-1273 COVID-19 Vaccine Efficacy Trial. *medRxiv* **2021**, 2021.08.09.21261290.
3. Lumley, S. F.; O'Donnell, D.; Stoesser, N. E.; Matthews, P. C.; Howarth, A.; Hatch, S. B.; Marsden, B. D.; Cox, S.; James, T.; Warren, F.; Peck, L. J.; Ritter, T. G.; de Toledo, Z.; Warren, L.; Axten, D.; Cornall, R. J.; Jones, E. Y.; Stuart, D. I.; Screaton, G.; Ebner, D.; Hoosdally, S.; Chand, M.; Crook, D. W.; O'Donnell, A.-M.; Conlon, C. P.; Pouwels, K. B.; Walker, A. S.; Peto, T. E. A.; Hopkins, S.; Walker, T. M.; Jeffery, K.; Eyre, D. W., Antibody Status and Incidence of SARS-CoV-2 Infection in Health Care Workers. *New England Journal of Medicine* **2020,** *384* (6), 533-540.
4. Tartof, S. Y.; Slezak, J. M.; Fischer, H.; Hong, V.; Ackerson, B. K.; Ranasinghe, O. N.; Frankland, T. B.; Ogun, O. A.; Zamparo, J. M.; Gray, S.; Valluri, S. R.; Pan, K.; Angulo, F. J.; Jodar, L.; McLaughlin, J. M., Effectiveness of mRNA BNT162b2 COVID-19 vaccine up to 6 months in a large integrated health system in the USA: a retrospective cohort study. *The Lancet* **2021,** *398* (10309), 1407-1416.
5. Goldberg, Y.; Mandel, M.; Bar-On, Y. M.; Bodenheimer, O.; Freedman, L.; Haas, E. J.; Milo, R.; Alroy-Preis, S.; Ash, N.; Huppert, A., Waning immunity of the BNT162b2 vaccine: A nationwide study from Israel. *medRxiv* **2021**, 2021.08.24.21262423.
6. Mizrahi, B.; Lotan, R.; Kalkstein, N.; Peretz, A.; Perez, G.; Ben-Tov, A.; Chodick, G.; Gazit, S.; Patalon, T., Correlation of SARS-CoV-2 Breakthrough Infections to Time-from-vaccine; Preliminary Study. *medRxiv* **2021**, 2021.07.29.21261317.
7. Naaber, P.; Tserel, L.; Kangro, K.; Sepp, E.; Jürjenson, V.; Adamson, A.; Haljasmägi, L.; Rumm, A. P.; Maruste, R.; Kärner, J.; Gerhold, J. M.; Planken, A.; Ustav, M.; Kisand, K.; Peterson, P., Dynamics of antibody response to BNT162b2 vaccine after six months: a longitudinal prospective study. *The Lancet Regional Health – Europe* **2021**, 10.1016/j.lanepe.2021.100208.
8. Piotr, K.; Dorota, K.; Anna, H.; Robert, M.; Samuel, S.; Anna, S.-B., Systemic COVID-19 vaccination also enhances the humoral immune response after SARS CoV-2 infection. An approach to criteria for COVID-19 reimmunization is needed. Do we need a third dose? *Research Square* **2021**, 10.21203/rs.3.rs-858160/v1
9. Goel, R. R.; Apostolidis, S. A.; Painter, M. M.; Mathew, D.; Pattekar, A.; Kuthuru, O.; Gouma, S.; Hicks, P.; Meng, W.; Rosenfeld, A. M., Distinct antibody and memory B cell responses in SARS-CoV-2 naïve and recovered individuals after mRNA vaccination. *Science immunology* **2021,** *6* (58), eabi6950.
10. Cromer, D.; Steain, M.; Reynaldi, A.; Schlub, T. E.; Wheatley, A. K.; Juno, J. A.; Kent, S. J.; Triccas, J. A.; Khoury, D. S.; Davenport, M. P., SARS-CoV-2 variants: levels of neutralisation required for protective immunity. *medRxiv* **2021**, 2021.08.11.21261876, https://doi.org/10.1101/2021.08.11.21261876.
11. Khoury, D. S.; Cromer, D.; Reynaldi, A.; Schlub, T. E.; Wheatley, A. K.; Juno, J. A.; Subbarao, K.; Kent, S. J.; Triccas, J. A.; Davenport, M. P., Neutralizing antibody levels are highly

predictive of immune protection from symptomatic SARS-CoV-2 infection. *Nature Medicine* **2021,** *27* (7), 1205-1211.
12. Williams, D. E., Importation Risk Stratification for COVID19 using Quantitative Serology. *medRxiv* **2021**, 2021.09.29.21264323.
13. Murin, C. D.; Wilson, I. A.; Ward, A. B., Antibody responses to viral infections: a structural perspective across three different enveloped viruses. *Nature microbiology* **2019,** *4* (5), 734-747.
14. Maginnis, M. S., Virus-Receptor Interactions: The Key to Cellular Invasion. *J Mol Biol* **2018,** *430* (17), 2590-2611.
15. Mostaghimi, D.; Valdez, C. N.; Larson, H. T.; Kalinich, C. C.; Iwasaki, A., Prevention of host-to-host transmission by SARS-CoV-2 vaccines. *The Lancet Infectious Diseases* **2021**, https://doi.org/10.1016/S1473-3099(21)00472-2.
16. Tortorici, M. A.; Beltramello, M.; Lempp, F. A.; Pinto, D.; Dang, H. V.; Rosen, L. E.; McCallum, M.; Bowen, J.; Minola, A.; Jaconi, S., Ultrapotent human antibodies protect against SARS-CoV-2 challenge via multiple mechanisms. *Science* **2020,** *370* (6519), 950-957.
17. Ke, Z.; Oton, J.; Qu, K.; Cortese, M.; Zila, V.; McKeane, L.; Nakane, T.; Zivanov, J.; Neufeldt, C. J.; Cerikan, B.; Lu, J. M.; Peukes, J.; Xiong, X.; Kräusslich, H.-G.; Scheres, S. H. W.; Bartenschlager, R.; Briggs, J. A. G., Structures and distributions of SARS-CoV-2 spike proteins on intact virions. *Nature* **2020,** *588* (7838), 498-502.
18. Laue, M.; Kauter, A.; Hoffmann, T.; Möller, L.; Michel, J.; Nitsche, A., Morphometry of SARS-CoV and SARS-CoV-2 particles in ultrathin plastic sections of infected Vero cell cultures. *Scientific Reports* **2021,** *11* (1), 3515.
19. Ishida, K., Stochastic Model for Langmuir Isotherm. *Bulletin of the Chemical Society of Japan* **1969,** *42* (2), 563-564.
20. Boulant, S.; Stanifer, M.; Lozach, P.-Y., Dynamics of virus-receptor interactions in virus binding, signaling, and endocytosis. *Viruses* **2015,** *7* (6), 2794-2815.
21. Schmidt, F.; Weisblum, Y.; Rutkowska, M.; Poston, D.; Silva, J. D.; Zhang, F.; Bednarski, E.; Cho, A.; Schaefer-Babajew, D. J.; Gaebler, C.; Caskey, M.; Nussenzweig, M. C.; Hatziioannou, T.; Bieniasz, P. D., High genetic barrier to escape from human polyclonal SARS-CoV-2 neutralizing antibodies. *bioRxiv* **2021**, 2021.08.06.455491.
22. Ainsworth, M.; Andersson, M.; Auckland, K.; Baillie, J. K.; Barnes, E.; Beer, S.; Beveridge, A.; Bibi, S.; Blackwell, L.; Borak, M., Performance characteristics of five immunoassays for SARS-CoV-2: a head-to-head benchmark comparison. *The Lancet Infectious Diseases* **2020,** *20* (12), 1390-1400.
23. Roche Canadian package insert: Roche-Anti-SARS-CoV-2-S-09203095190-EN-Can.pdf https://www.rochecanada.com/en/products/diagnostics-products/documentation/canadian-package-inserts.html (accessed 24 October 2021).
24. Wei, J.; Stoesser, N.; Matthews, P. C.; Ayoubkhani, D.; Studley, R.; Bell, I.; Bell, J. I.; Newton, J. N.; Farrar, J.; Diamond, I.; Rourke, E.; Howarth, A.; Marsden, B. D.; Hoosdally, S.; Jones, E. Y.; Stuart, D. I.; Crook, D. W.; Peto, T. E. A.; Pouwels, K. B.; Eyre, D. W.; Walker, A. S.; Team, C.-I. S., Antibody responses to SARS-CoV-2 vaccines in 45,965 adults from the general population of the United Kingdom. *Nature Microbiology* **2021**, 10.1038/s41564-021-00947-3.
25. Shrotri, M.; Fragaszy, E.; Geismar, C.; Nguyen, V.; Beale, S.; Braithwaite, I.; Byrne, T. E.; Fong, W. L. E.; Kovar, J.; Navaratnam, A., Spike-antibody responses to ChAdOx1 and BNT162b2 vaccines by demographic and clinical factors (Virus Watch study). *medRxiv* **2021**, https://doi.org/10.1101/2021.05.12.21257102; .